Towards Transformer-Based Aligned Generation with Self-Coherence Guidance

Shulei Wang^{1*} Wang Lin^{1*} Hai Huang¹ Hanting Wang¹ Sihang Cai¹ WenKang Han¹ Tao Jin¹ Jingyuan Chen¹ Jiacheng Sun² Jieming Zhu² Zhou Zhao^{1†}

¹ Zhejiang University ² Huawei Noah's Ark Lab

shuleiwang@zju.edu.cn, zhaozhou@zju.edu.cn



Figure 1. Our method directly optimizes the cross-attention maps in Transformer-based diffusion models, significantly enhancing the model's performance in coarse-grained attribute binding and further improving fine-grained attribute and style binding. For instance, our approach enables precise control over the color of an apple's flesh and stem as well as the style of two distinct concepts.

Abstract

We introduce a novel, training-free approach for enhancing alignment in Transformer-based Text-Guided Diffusion Models (TGDMs). Existing TGDMs often struggle to generate semantically aligned images, particularly when dealing with complex text prompts or multi-concept attribute binding challenges. Previous U-Net-based methods primarily optimized the latent space, but their direct application to Transformer-based architectures has shown limited effectiveness. Our method addresses these challenges by directly optimizing cross-attention maps during the generation process. Specifically, we introduce Self-Coherence Guidance, a method that dynamically refines attention maps using masks derived from previous denoising steps, ensuring

precise alignment without additional training. To validate our approach, we constructed more challenging benchmarks for evaluating coarse-grained attribute binding, fine-grained attribute binding, and style binding. Experimental results demonstrate the superior performance of our method, significantly surpassing other state-of-the-art methods across all evaluated tasks. Our code is available at https://scg-diffusion.github.io/scg-diffusion.

1. Introduction

Text-guided diffusion models (TGDMs) [38, 40, 42] have demonstrated significant capability, generating high-quality images based on given textual prompts. Previous mainstream TGDMs [40, 42] have primarily utilized the U-Net architecture [41], predicting noise through down-sampling and up-sampling modules. Recently, Transformer [47], due to its robustness [48], scalability [35], and efficient modality fusion [11, 18, 19], has been widely applied in large language models(LLMs) [2, 33, 46] and multi-modal large language models(LLMs) [35].

^{*}Equal contribution.

[†]Corresponding author

guage models(MLLMs) [22, 30, 53].

Peebles *et al.* [35] were the first to explore the use of transformers in generative tasks. This pioneering work was followed by several subsequent works [7, 8, 24] that have enabled high-quality image generation and demonstrated strong scalability.

Aligned generation is a challenging task that requires the generated images and text to maintain a high level of alignment [15, 16, 51]. Nonetheless, we observe that the existing TGDMs, whether based on U-Net or Transformer architectures, struggle to maintain precise alignment, especially for complex prompts. We categorize these semantic discrepancies as follows:

- a) Coarse-grained attribute binding: For instance, as shown in Fig. 1(a), when prompted with "a red bench and an yellow clock", the model may incorrectly assign attributes to concepts, potentially mixing attributes between them.
- **b**) Fine-grained attribute binding: When referring to a specific part of a concept, the model may misattribute details. For example, as shown in Fig. 1(b), if prompted with "an apple with a blue fruit and an orange stem", the model may fail to apply the colors correctly to the intended parts. **c**) Style binding: When required to generate multiple concepts in distinct styles, as shown in Fig. 1(c), the model may incorrectly assign styles to concepts, leading to misaligned visual outcomes.

Previous work has explored aligned generation based on U-Net models, but these methods show limited effectiveness when applied to Transformer-based models, as shown in Fig.4. Therefore, we revisited the differences between the U-Net and Transformer architectures, as illustrated in Fig.6. Our findings indicate that in Transformer-based architectures, it is more challenging to identify attention maps with strong core semantic information to guide the latent generation process.

Therefore, we delve deeper into the Transformer-based framework to address these three challenges. Upon closely analyzing the Transformer-based architecture, We find that, due to the absence of downsampling and upsampling modules in the Transformer architecture, the shape of the crossattention maps during the generation process remains unchanged. This property provides us with the convenience of directly operating the cross-attention maps. Can we directly optimize the maps during the generation process in the same way as the cross attention editing [13]? The answer is no. This is because the cross attention editing is designed for image editing task, where an existing generated image guides the creation of another image. In contrast, direct text-to-image generation relies solely on text as guidance, without an additional image to guide the process. So we propose a training-free, self-coherence guidance approach for cross-attention maps. Specifically, we dynamically extract masks from the previous denoising step's features, then apply these masks to refine the current step's attention map for enhanced alignment.

To validate the effectiveness of our method, we constructed a more challenging benchmark for fine-grained attribute and style binding, building upon previous attribute-binding benchmarks. We conducted comprehensive evaluations of the generated results, including qualitative and quantitative assessments, as well as a user study. To summary, our main contributions are as follows:

- We propose a novel, training-free approach for transformer-based TGDMs that directly optimizes the cross attention map rather than the latent representation.
- To validate our approach, we introduce more challenging benchmarks, evaluating not only simple coarse-grained attribute binding but also fine-grained attribute binding and style binding.
- Extensive experiments verify the effectiveness of our method, demonstrating superior performance over baselines and state-of-the-art U-Net-based methods.

2. Related work

2.1. Text-Guided Diffusion Model

TGDMs [40, 42], such as Stable Diffusion(SD) [40] and Imagen [42], have demonstrated remarkable capabilities by generating high-quality images from given textual prompts. Current mainstream TGDMs generally fall into two categories: those based on U-Net architectures and those based on Transformer architectures. Previous SOTA models have primarily utilized the U-Net-based approach, as seen in models like Stable Diffusion [40]. However, the successful application of transformers in large language models and multimodal models has highlighted their significant advantages. Recently, Peebles et al. [35] proposed DiT, a fully Transformer-based architecture, which showcases greater scalability. PixArt- α [7] further advances this approach by incorporating a multi-head cross-attention mechanism that bridges the text and image modalities, allowing high-quality image generation with reduced training data requirements.

2.2. Aliged generation

Despite the remarkable success of diffusion models in text-to-image generation, even state-of-the-art models, such as Stable Diffusion, struggle to generate images that highly align with text prompts [6, 9, 28, 29, 44, 49], particularly when dealing with complex semantics or attribute binding. Consequently, a range of methods [3, 5, 14, 20, 25, 39, 50, 54] has been proposed to improve alignment in pre-trained diffusion T2I models. Current approaches can be categorized into two main types: those requiring fine-tuning and those that are training-free.

Fine-tuning Methods: Methods requiring fine-tuning often involved lightweight adjustments or multimodal

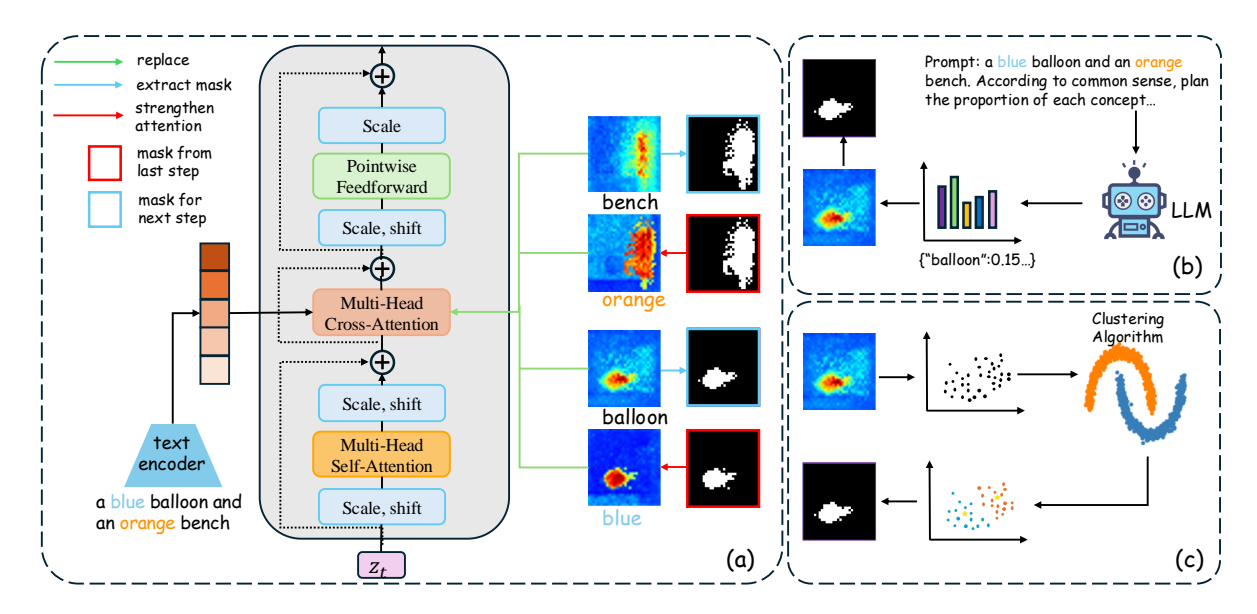


Figure 2. (a) Overview of our method. Given a prompt, we extract the corresponding concept masks and use these masks to directly guide the attribute or style maps. (b) For fine-grained attribute binding, we extract masks by planning the proportions using LLMs. (c) For coarse-grained attribute binding and style binding, we directly apply clustering methods to extract the corresponding masks.

alignment to enhance control over generation. For instance, Mou *et al.* [32] introduced a lightweight adapter that allowed for rich control of the generated results. Feng *et al.* [10] incorporated a semantic panel to decouple T2I tasks into "text-to-semantic panel" and "semantic panel-to-image" processes and constructed a relevant dataset for model fine-tuning, thereby achieving aliged generation. Shen *et al.* [43] employed a scene graph adapter to deconstruct text into scene graphs, enabling SD to capture semantic relationships [26, 27] more effectively.

Training-Free Methods: Training-free approaches [6, 12, 23, 31, 52, 55] typically optimized the inference process directly, avoiding the computational demands and potential issues like catastrophic forgetting associated with fine-tuning. Chefer *et al.* [6] introduced Generative Semantic Nursing, using features from the generation process to guide latent generation by activating concept tokens in the cross-attention map; however, it did not fully resolve attribute binding issues. Li *et al.* [23] further designed a binding loss to align color and concept cross-attention maps more closely. Meral *et al.* [31] leveraged contrastive learning to achieve promising results by pushing apart mismatched attribute-concept pairs and pulling closer matched attribute-concept pairs.

While these methods have improved generation alignment to some extent, they remain limited in handling fine-grained attribute and style bindings. Notably, previous training-free approaches optimize the latent space, whereas our method directly optimizes the cross-attention map. This not only improves coarse-grained attribute binding but also enables precise fine-grained attribute and style binding.

3. Methodology

In this section, we begin by introducing the concept of TGDMs and denoising network, followed by a detailed presentation of our proposed method for directly optimizing the attention map. The framework of our approach is illustrated in Fig. 2

3.1. Preliminaries

Text-Guided Diffusion Models Our method is primarily based on the text-guided diffusion model. Existing approaches usually operate predominantly in the latent space rather than at the pixel level. Specifically, a Variational Autoencoder(VAE) includes an encoder $\mathcal E$ that encodes an input image x into a lower-dimensional latent code z, and a decoder $\mathcal D$ that reconstructs z back into the original image $\mathcal D(z) \approx x$. Normally, the VAE remains fixed during the training of the denoising network .

In detail, noise ϵ is gradually added to the initial latent z_0 to produce a noisy latent representation z_t , and a denoising network ϵ_{θ} is trained to predict the noise added to z_0 . The specific training objective is formulated as follows:

$$\mathcal{L} = \mathbb{E}_{z \sim \mathcal{E}(x), \epsilon \sim N(0, I), c, t} \left[\left\| \epsilon - \epsilon_{\theta} \left(z_{t}, c, t \right) \right\|^{2} \right]$$
 (1)

Here, c denotes conditional information, specifically referring to the text input. During inference, we begin by randomly sampling z_t from a Gaussian distribution. The denoising network iteratively estimates and removes noise from z_t based on both z_t and the condition c, ultimately obtaining the clean latent code z_0 . By operating within the



Figure 3. Qualitative analysis of our method compared to other SOTA methods. Our approach consistently generates high-quality images with superior alignment across coarse-grained attribute binding, fine-grained attribute binding, and style binding tasks.

latent space, this approach enables more efficient and robust image synthesis.

Denoising Network ϵ_{θ} in TGDMs Current denoising networks can be broadly categorized into two types: U-Net-based and Transformer-based models. U-Net-based denoising networks leverage convolutional neural networks (CNNs), while Transformer-based models are entirely built upon attention mechanisms. In Transformer-based TGDMs architectures, there are typically n Transformer blocks, each consisting of a self-attention module and a cross-attention module. In the self-attention module, latent features are encoded as Q, K, and V. The attention weights are computed using the following equation: Attention(Q, K, V) =softmax $\left(\frac{QK^{\top}}{\sqrt{d_k}}\right)V$. In the cross-attention module, text embeddings—typically generated by a frozen text encoder [36, 37]—are encoded as K, and V vectors by the crossattention layer, enabling the integration of text-based conditional information.while the hidden states from the transformer block are projected to generate the Q vectors. Using the formula $A_t = \operatorname{Softmax}\left(\frac{QK^T}{\sqrt{d}}\right)$, where t denotes the time step, we obtain the cross-attention map. The softmax operation is performed along the final dimension. To more intuitively represent the semantic information of the crossattention map, we typically reshape A_t into dimensions $\mathbb{R}^{h \times w \times L}$, where h, w denote the spatial dimensions of the map, and l represents the length of the text sequence. The attention map for the s-th token is denoted as A_t^s . It is noted that both U-Net-based models and Transformer-based models have cross-attention maps, and Prompt-to-Prompt [13] demonstrates that cross-attention maps contains rich semantic information, which plays a critical role in determining the content of the generated image.

3.2. Self-Coherence Guidance

Our purpose is to enhance the performance of Transformer-based TGDMs in aligned generation. To achieve this, we first compare the differences between Transformer-based and U-Net-based architectures. Intuitively, there is a significant structural difference: the Transformer architecture does not include upsampling and downsampling modules. As a result, the hidden state shape remains constant across all layers, and the shape of the cross-attention map remains unchanged.

Upon deeper investigation, we observe differences in their behavior during the generation process. As illustrated in Fig. 6, the Transformer-based TGDMs exhibit more evenly distributed semantic information in the crossattention map during generation, making it more difficult to identify the core map.

Inspired by the cross attention editing [13], which has shown impressive results in image editing tasks, we rec-

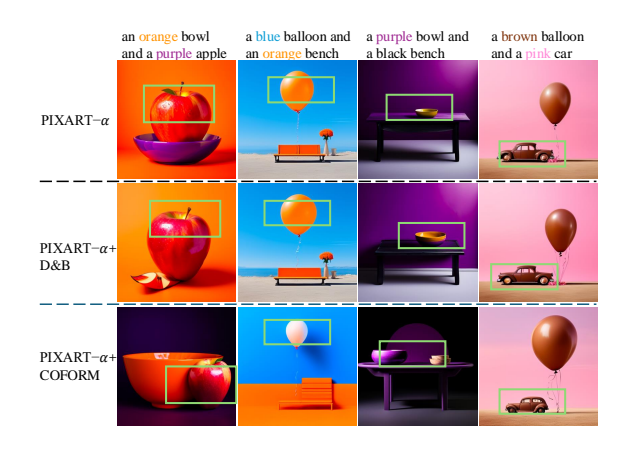


Figure 4. Qualitative results of directly transferring D&B and CONFORM methods to Transformer-based architectures.

ognize that this mechanism requires a reference image's cross-attention map as guidance. However, our task involves direct text-to-image generation without a reference image. Therefore, based on the above analysis, we propose the Self-Coherence Guidance, with the core idea being to directly optimize the maps during the generation process.

Specifically, TGDMs can generate different parts of two concepts or a single concept. It knows "what to draw", but not "where to draw" it [34, 45], leading to errors in attribute binding. For instance, when the prompt is "a blue balloon and an orange bench" or "an apple with blue flesh and a red stem", TGDMs can generally generate complete parts of the balloon, bench, and apple. However, it often assigns incorrect colors to the corresponding parts.

Therefore, we can leverage the prior knowledge that TGDM knows "what to draw" to implement self-coherence guidance.

We denote concept tokens as o and attribute or style tokens as r at step t, where z_t generates z_{t-1} , we leverage the concept tokens at step t+1 (such as balloon, stem, etc.) to extract a mask $M_{t+1}^{o_i}$ and directly enhance A_t . To achieve this enhancement, we define the following update rule for $\widehat{A_t}$:

$$\left(\widehat{A_t}\right)_{p,q} := \begin{cases} c \cdot (A_t)_{p,q} & \text{if } q = r_i \text{ and } M_{t+1}^{o_i}[p] == 1, \\ (A_t)_{p,q} & \text{otherwise.} \end{cases}$$
 (2)

Here, p represents a position index within the cross-attention map, q denotes a token index, and i indicates the index of an concept-attribute pair.

To obtain $M_{t+1}^{o_i}$, we first average the attention maps across all layers at step t+1 and then adopt different methods depending on the specific task. For coarse-grained attribute binding and style binding, we directly apply the K-means algorithm to the averaged cross-attention map, dividing it into two categories to generate the mask. For fine-grained attribute binding, although the cross-attention map can still focus on the corresponding regions, clustering fails

to effectively capture the detailed concepts. To address this, we leverage LLMs to determine the proportions. Specifically, given a prompt such as "an apple with blue flesh and an orange stem", we query LLMs to leverage its commonsense reasoning and infer the approximate ratio of the flesh and stem regions in an image of an apple. Based on the inferred ratio, we extract the mask by selecting regions in the cross-attention map whose values fall within the top proportion corresponding to the calculated ratio.

Then, we calculate $\widehat{A_t}$ using Equation (2) and replace the original A_t with $\widehat{A_t}$ to directly guide the diffusion model in generating images that closely align with the text.

4. Experiments

Our method addresses challenges in Coarse-grained attribute binding, Fine-grained attribute binding, and Style binding in Transformer-based TGDMs. Our experiments are designed to address the following research questions:

- **RQ1**: Can the previously proposed training-free disambiguation method based on U-Net be directly applied to Transformer-based models?
- **RQ2**: Can existing training-free disambiguation methods be extended to broader applications, such as fine-grained attribute binding and style binding?
- **RQ3**: Is Self-Coherence Guidance effective across all three scenarios?

Experimental setup Existing benchmarks typically focus on evaluating coarse-grained attribute binding, but lack benchmarks and prompts for fine-grained attribute and style binding. For coarse-grained attribute binding, we adopt the prompts from prior work. However, upon analysis, we found that these structured prompts lack diversity and are not adapted to specific scenes. For example, they lack prompts like "a [colorA] [animal] and a [colorB] [object]" or "a [colorA] [animal] and a [colorB] [object] in the kitchen." Therefore, based on previous work [6], we constructed a more challenging coarse-grained attribute binding benchmark using manually created prompts, enhancing prompt complexity. Additionally, we developed fine-grained attribute binding and style binding structured prompts for quantitative and qualitative analysis through a similar manual construction approach.

Specifically, the structure of the prompt for coarse-grained attribute binding is "a [colorA] [objectA] and a [colorB] [objectB]", "a [colorA] [animal] and a [colorB] [object]", "a [colorA] [animal] and a [colorB] [object] in the [place]". For fine-grained attribute binding, the prompt structure is "an object with a [colorA] [partA] and a [colorB] [partB]". For style binding, the prompt structure is "a [styleA] [objectA] and a [styleB] [objectB]". The details of the benchmark can be found in the supplementary material.

We conduct experiments on PIXART- α -512. For each

Table 1. Comparison of image-text similarity and text-text similarity for the direct transfer of U-Net-based methods to Transformer-based models.

Method	image-text	text-text
PIXART- α [7]	0.36	0.807
w/ D&B [23]	0.35	0.807
w/ CONFORM [31]	0.36	0.814
SD [40]	0.34	0.771
w/ D&B [23]	0.36	0.803
w/ CONFORM [31]	0.36	0.824



Figure 5. Generation results of U-Net-based CONFORM using cross-attention maps at different resolutions, where the results at corresponding positions are generated using the same random seed. The text prompt is "a purple dog and a green bench".

prompt, we use 64 different random seeds with 50 iterations. The parameter c is set to 4.

Baselines To investigate the generation alignment challenges within Transformer-based architectures, we conduct experiments on the text-to-image model PIXART- α [7], which is based on the DiT architecture. Our baselines include the original PIXART- α , Divide & Bind (D&B) [23], and CONFORM [31]. It is worth noting that both D&B and CONFORM are state-of-the-art training-free methods specifically designed for U-Net-based models. Initially, we simply adapt these U-Net-based SOTA methods to the transformer-based PIXART- α model. To further demonstrate the remarkable effectiveness of our method in addressing generation consistency and to explore the upper bounds of our method's performance, we also compare it with the original U-Net-based SOTA methods, all of which are based on Stable Diffusion v1.5 and have demonstrated strong capabilities in various scenarios.

4.1. Direct Transfer of U-Net-Based Methods to Transformer-Based model(RQ1)

We begin by directly applying the D&B [23] and CON-FORM [31] methods to PIXART- α , following the original parameter configurations to conduct experiments on a original objects binding benchmark [6].

Qualitative Results Figure 4 illustrates the experimental results of PIXART- α and the direct application of D&B and CONFORM to PIXART- α , with each method using the

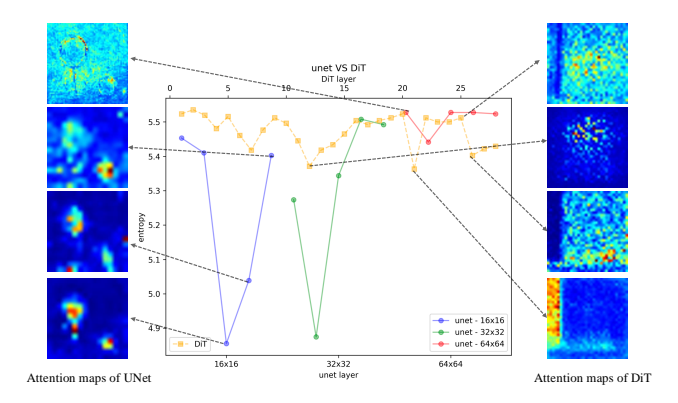


Figure 6. During the generation process, the attention entropy across different layers in U-Net and DiT architectures reflects the semantic richness, with lower attention entropy indicating greater semantic information. The visualized token corresponds to the word "balloon".

same seed. Neither D&B nor CONFORM effectively addresses the attribute binding issues in Transformer-based architectures. We summarize the challenges of directly transferring U-Net-based methods into three main areas. (a): Difficulty in achieving full attribute binding, often resulting in only one attribute being correctly bound. For instance, when the prompt is "an orange bowl and a purple apple", CONFORM correctly binds the color orange to the bowl but fails to bind purple to the apple. (b): Reduced generation quality. As shown in the Fig. 4, both D&B and CONFORM can result in incomplete or malformed concepts. (c): Potential for decreased semantic alignment. For example, when the prompt is "a purple bowl and a black bench", PIXART- α successfully generates a bowl and a bench, but CONFORM generates an additional bowl, as illustrated in the Fig. 4.

Quantitative Results To further investigate the effects of directly applying D&B and CONFORM, we conducted a quantitative analysis of the generated results using several metrics. We assessed image-text similarity and textext similarity. Following previous methodologies, we used CLIP [36] to separately encode the image and text, then calculated their similarity. Additionally, we employed the BLIP model [21] to generate captions for the images, subsequently calculating the similarity between the generated caption and the text prompt.

As shown in the table 1, while the use of the CONFORM method improves text-text similarity compared to PIXART- α , it still lags behind the performance of the SD-based Conform approach. This suggests that directly applying U-Netbased methods yields limited effectiveness.

The limited effectiveness of directly applying U-Netbased methods to Transformer architectures motivates us to explore the underlying causes. Through an analysis of both U-Net and Transformer architectures, we have identified the following insights: due to the presence of downsam-

Table 2. Comparison of average text-text similarity, demonstrating that our method outperforms other baselines across all three subtasks. Green represents the best results, while blue indicates the second-best results.

Method	Coarse-grained Fine-grained		Style
D&B(SD) [23]	0.798	0.742	0.660
CONFORM(SD) [31]	0.834	0.774	0.642
PIXART- α [7]	0.808	0.804	0.688
Ours	0.852	0.827	0.689

Table 3. Comparison of BLIP-VQA scores. Our method also demonstrates state-of-the-art performance, significantly surpassing the original PIXART- α model in both coarse-grained and finegrained attribute binding.

Method	Coarse-grained	Fine-grained	Style
D&B(SD) [23]	0.499	0.451	0.514
CONFORM(SD) [31]	0.667	0.522	0.498
PIXART- α [7]	0.293	0.398	0.676
Ours	0.679	0.623	0.799

pling and upsampling modules within the U-Net architecture, it produces cross-attention maps at varying resolutions. Among these, the 16x16 resolution maps are particularly notable for capturing richer semantic information [13, 31]. Consequently, many U-Net-based methods tend to leverage the 16x16 cross-attention map.

To further verify whether the semantic information at 16x16 is indeed stronger, we set the resolution in CONFORM to 16, 32, and 64, respectively. As shown in the Figure 5, generation quality is superior when the resolution is set to 16, while it significantly degrades at 32 and 64, indicating that the 16x16 cross-attention map does contain richer semantic information. To quantitatively compare the semantic information in U-Net and Transformer, we visualized the entropy [4] of the cross-attention maps for each layer. Lower entropy reflects stronger semantic information. As illustrated in the Figure 6, the overall semantic strength is higher in U-Net's 16x16 maps during generation. Although entropy decreases slightly in the final layers of DiT, the trend remains relatively stable throughout.

When directly adapting U-Net-based methods, the inherent characteristics of the Transformer—where all cross-attention maps share the same resolution and semantic information is more evenly distributed throughout the generation process—limit our ability to identify a core map with distinctly stronger semantic features.

Moreover, U-Net-based SOTA methods extract features via cross-attention and apply loss functions (e.g., contrastive or JS divergence) to guide latents, introducing an inherent gap that is aggravated by the relatively low semantic consistency of Transformer-based attention maps.

4.2. Self-Coherence Guidance VS U-Net-based SOTA methods (RQ2, RQ3)

The suboptimal outcomes observed when directly transferring U-Net-based methods to Transformer architectures have motivated us to seek a more effective solution. We propose a novel paradigm that leverages the prior knowledge of generative models to directly optimize cross-attention maps. This approach bypasses the inherent gap introduced by previous U-Net-based methods, which typically involve an intermediate step of extracting cross-attention map features, calculating a loss, and subsequently optimizing the latent space towards the desired direction. By avoiding this intermediate step, our method achieves improved results.

Qualitative Results As shown in the Fig. 3, we compare our results with the original PIXART- α , SD-based D&B, and SD-based CONFORM. All methods were evaluated using the same seed for consistency. We observe that: (a) In the traditional coarse-grained attribute binding task, our method not only generates images with high consistency with the text prompts but also achieves state-of-the-art generation coherence. Although CONFORM also demonstrates competitive consistency, it sacrifices image quality. In contrast, our method maintains high fidelity in the generated images while preserving alignment. (b) Previous methods have struggled to precisely control specific parts of a concept at a fine-grained level. For example, when given the prompt "a sunflower with blue petals and a yellow stem", other methods either confuse the colors of different parts or separate the two parts of the concept, failing to maintain the intended semantics of the prompt. Our approach, however, successfully controls the color of each part, generating high-quality, highly aligned images. (c) In the style-binding task, we aim for the model to control the style of two distinct concepts independently. For instance, we may want Spider-Man in a realistic style and the background in an Impressionist style. We observe that previous methods fail to manage different styles for separate concepts, often resulting in subpar outputs. In contrast, our method achieves successful style binding.

Quantitative Results We use text-text similarity and BLIP-VQA as evaluation metrics. When evaluating text-text similarity, we first generate captions for images using BLIP. However, the BLIP captioning model does not always describe detailed attributes of each concept [17]. Therefore, Huang *et al.* [17] proposes BLIP-VQA, which decouples complex text prompts into independent questions. Specifically, for an image generated from the prompt "a purple dog and a green bench", two separate questions are asked: "a purple dog?" and "a green bench?"

As shown in the table 2, our method consistently outperforms other baselines in text-text similarity evaluation. Although it achieves only a slight improvement over the origi-

Table 4. User study with 50 participants

Method	Coarse-grained Fine-grained		Style
D&B(SD) [23]	3.2%	0.6%	1.4%
CONFORM(SD) [31]	13.2%	4.6%	0.4%
PIXART- α [7]	2.6%	4.2%	5.6%
Ours	81%	90.6%	92.6%

nal PIXART- α in style binding, we attribute this to a limitation in the BLIP-caption model: when generating captions, BLIP struggles to accurately capture the distinct styles of each concept, which reduces the text-text similarity score.

As shown in the table 3, in the BLIP-VQA evaluation, our method also surpasses the original PIXART- α and other U-Net-based SOTA methods across all three subsets. Notably, the original PIXART- α model performs worse than the U-Net-based SOTA methods in both coarse binding and fine binding tasks, further underscoring the necessity of exploring generation consistency within Transformer-based architectures. Our method significantly enhances the original PIXART- α model, achieving substantial improvements in coarse binding and a 56% increase in fine binding, which strongly demonstrates the effectiveness of our approach. In style binding, while the original PIXART- α model also performs well, our method effectively leverages its prior knowledge, further extending its capabilities and achieving an 18% improvement.

User study To further evaluate the generation quality of our method, we conducted a comprehensive user study involving 50 participants. Specifically, following the setup of previous methods [6], we randomly selected 10 prompts for each subtask and generated images using each method with the same random seed. Similarly, we asked participants to select the image that best matched the text prompt from those generated by different methods. We used the frequency of selection as the evaluation metric. Table 4 presents the results of our user study, showing that users consistently preferred the images generated by our method across all three tasks. This strong user preference highlights the effectiveness of our approach.

5. Conclusions

In this work, we proposed a training-free Self-Coherence Guidance method to address alignment challenges in Transformer-based TGDMs. By directly optimizing cross-attention maps rather than latent spaces, our approach effectively improves coarse-grained, fine-grained, and style binding tasks, surpassing the performance of existing state-of-the-art methods. Our findings underscore the potential of leveraging attention map optimization as a pathway for addressing alignment issues, paving the way for future advancements in TGDMs.

References

- [1] Flux. https://github.com/black-forestlabs/flux/, 2024. 3
- [2] Josh Achiam, Steven Adler, Sandhini Agarwal, Lama Ahmad, Ilge Akkaya, Florencia Leoni Aleman, Diogo Almeida, Janko Altenschmidt, Sam Altman, Shyamal Anadkat, et al. Gpt-4 technical report. arXiv preprint arXiv:2303.08774, 2023. 1
- [3] Aishwarya Agarwal, Srikrishna Karanam, KJ Joseph, Apoorv Saxena, Koustava Goswami, and Balaji Vasan Srinivasan. A-star: Test-time attention segregation and retention for text-to-image synthesis. In *Proceedings of the IEEE/CVF International Conference on Computer Vision*, pages 2283– 2293, 2023. 2
- [4] Giuseppe Attanasio, Debora Nozza, Dirk Hovy, and Elena Baralis. Entropy-based attention regularization frees unintended bias mitigation from lists. *arXiv preprint arXiv:2203.09192*, 2022. 7
- [5] Zhipeng Bao, Yijun Li, Krishna Kumar Singh, Yu-Xiong Wang, and Martial Hebert. Separate-and-enhance: Compositional finetuning for text-to-image diffusion models. In ACM SIGGRAPH 2024 Conference Papers, pages 1–10, 2024. 2
- [6] Hila Chefer, Yuval Alaluf, Yael Vinker, Lior Wolf, and Daniel Cohen-Or. Attend-and-excite: Attention-based semantic guidance for text-to-image diffusion models. ACM Transactions on Graphics (TOG), 42(4):1–10, 2023. 2, 3, 6, 8, 1
- [7] Junsong Chen, Jincheng Yu, Chongjian Ge, Lewei Yao, Enze Xie, Yue Wu, Zhongdao Wang, James Kwok, Ping Luo, Huchuan Lu, et al. Pixart-α: Fast training of diffusion transformer for photorealistic text-to-image synthesis. arXiv preprint arXiv:2310.00426, 2023. 2, 6, 7, 8, 3
- [8] Shoufa Chen, Mengmeng Xu, Jiawei Ren, Yuren Cong, Sen He, Yanping Xie, Animesh Sinha, Ping Luo, Tao Xiang, and Juan-Manuel Perez-Rua. Gentron: Delving deep into diffusion transformers for image and video generation. arXiv e-prints, pages arXiv-2312, 2023. 2
- [9] Weixi Feng, Xuehai He, Tsu-Jui Fu, Varun Jampani, Arjun Akula, Pradyumna Narayana, Sugato Basu, Xin Eric Wang, and William Yang Wang. Training-free structured diffusion guidance for compositional text-to-image synthesis. arXiv preprint arXiv:2212.05032, 2022. 2
- [10] Yutong Feng, Biao Gong, Di Chen, Yujun Shen, Yu Liu, and Jingren Zhou. Ranni: Taming text-to-image diffusion for accurate instruction following. In *Proceedings of* the IEEE/CVF Conference on Computer Vision and Pattern Recognition, pages 4744–4753, 2024. 3
- [11] Rohit Girdhar, Alaaeldin El-Nouby, Zhuang Liu, Mannat Singh, Kalyan Vasudev Alwala, Armand Joulin, and Ishan Misra. Imagebind: One embedding space to bind them all. In Proceedings of the IEEE/CVF Conference on Computer Vision and Pattern Recognition, pages 15180–15190, 2023.
- [12] Xiefan Guo, Jinlin Liu, Miaomiao Cui, Jiankai Li, Hongyu Yang, and Di Huang. Initno: Boosting text-to-image diffusion models via initial noise optimization. In *Proceedings of*

- the IEEE/CVF Conference on Computer Vision and Pattern Recognition, pages 9380–9389, 2024. 3
- [13] Amir Hertz, Ron Mokady, Jay Tenenbaum, Kfir Aberman, Yael Pritch, and Daniel Cohen-Or. Prompt-to-prompt image editing with cross attention control. *arXiv preprint* arXiv:2208.01626, 2022. 2, 5, 7
- [14] Xiwei Hu, Rui Wang, Yixiao Fang, Bin Fu, Pei Cheng, and Gang Yu. Ella: Equip diffusion models with llm for enhanced semantic alignment. *arXiv preprint arXiv:2403.05135*, 2024. 2
- [15] Hai Huang, Shulei Wang, and Yan Xia. Semantic residual for multimodal unified discrete representation. arXiv preprint arXiv:2412.19128, 2024. 2
- [16] Hai Huang, Yan Xia, Shengpeng Ji, Shulei Wang, Hanting Wang, Jieming Zhu, Zhenhua Dong, and Zhou Zhao. Unlocking the potential of multimodal unified discrete representation through training-free codebook optimization and hierarchical alignment. arXiv preprint arXiv:2403.05168, 2024.
- [17] Kaiyi Huang, Kaiyue Sun, Enze Xie, Zhenguo Li, and Xihui Liu. T2i-compbench: A comprehensive benchmark for open-world compositional text-to-image generation. Advances in Neural Information Processing Systems, 36:78723–78747, 2023. 8
- [18] Zihan Huang, Tao Wu, Wang Lin, Shengyu Zhang, Jingyuan Chen, and Fei Wu. Autogeo: Automating geometric image dataset creation for enhanced geometry understanding. arXiv preprint arXiv:2409.09039, 2024. 1
- [19] Shengpeng Ji, Ziyue Jiang, Wen Wang, Yifu Chen, Minghui Fang, Jialong Zuo, Qian Yang, Xize Cheng, Zehan Wang, Ruiqi Li, et al. Wavtokenizer: an efficient acoustic discrete codec tokenizer for audio language modeling. *arXiv* preprint arXiv:2408.16532, 2024. 1
- [20] Yunji Kim, Jiyoung Lee, Jin-Hwa Kim, Jung-Woo Ha, and Jun-Yan Zhu. Dense text-to-image generation with attention modulation. In *Proceedings of the IEEE/CVF International Conference on Computer Vision*, pages 7701–7711, 2023. 2
- [21] Junnan Li, Dongxu Li, Caiming Xiong, and Steven Hoi. Blip: Bootstrapping language-image pre-training for unified vision-language understanding and generation. In *Interna*tional conference on machine learning, pages 12888–12900. PMLR, 2022. 7
- [22] Junnan Li, Dongxu Li, Silvio Savarese, and Steven Hoi. Blip-2: Bootstrapping language-image pre-training with frozen image encoders and large language models. In *International conference on machine learning*, pages 19730–19742. PMLR, 2023. 2
- [23] Yumeng Li, Margret Keuper, Dan Zhang, and Anna Khoreva. Divide & bind your attention for improved generative semantic nursing. *ArXiv*, abs/2307.10864, 2023. 3, 6, 7, 8, 2
- [24] Zhimin Li, Jianwei Zhang, Qin Lin, Jiangfeng Xiong, Yanxin Long, Xinchi Deng, Yingfang Zhang, Xingchao Liu, Minbin Huang, Zedong Xiao, et al. Hunyuan-dit: A powerful multi-resolution diffusion transformer with fine-grained chinese understanding. arXiv preprint arXiv:2405.08748, 2024.
- [25] Youwei Liang, Junfeng He, Gang Li, Peizhao Li, Arseniy Klimovskiy, Nicholas Carolan, Jiao Sun, Jordi Pont-Tuset,

- Sarah Young, Feng Yang, et al. Rich human feedback for text-to-image generation. In *Proceedings of the IEEE/CVF Conference on Computer Vision and Pattern Recognition*, pages 19401–19411, 2024. 2
- [26] Wang Lin, Tao Jin, Wenwen Pan, Linjun Li, Xize Cheng, Ye Wang, and Zhou Zhao. Tavt: Towards transferable audiovisual text generation. In *Proceedings of the 61st Annual Meeting of the Association for Computational Linguistics* (Volume 1: Long Papers), pages 14983–14999, 2023. 3
- [27] Wang Lin, Tao Jin, Ye Wang, Wenwen Pan, Linjun Li, Xize Cheng, and Zhou Zhao. Exploring group video captioning with efficient relational approximation. In *Proceedings of* the IEEE/CVF International Conference on Computer Vision, pages 15281–15290, 2023. 3
- [28] Wang Lin, Jingyuan Chen, Jiaxin Shi, Zirun Guo, Yichen Zhu, Zehan Wang, Tao Jin, Zhou Zhao, Fei Wu, YAN Shuicheng, et al. Action imitation in common action space for customized action image synthesis. In *The Thirty-eighth Annual Conference on Neural Information Processing Systems*, 2024. 2
- [29] Wang Lin, Jingyuan Chen, Jiaxin Shi, Yichen Zhu, Chen Liang, Junzhong Miao, Tao Jin, Zhou Zhao, Fei Wu, Shuicheng Yan, et al. Non-confusing generation of customized concepts in diffusion models. arXiv preprint arXiv:2405.06914, 2024. 2
- [30] Haotian Liu, Chunyuan Li, Qingyang Wu, and Yong Jae Lee. Visual instruction tuning. *Advances in neural information processing systems*, 36, 2024. 2
- [31] Tuna Han Salih Meral, Enis Simsar, Federico Tombari, and Pinar Yanardag. Conform: Contrast is all you need for high-fidelity text-to-image diffusion models. In *Proceedings of the IEEE/CVF Conference on Computer Vision and Pattern Recognition*, pages 9005–9014, 2024. 3, 6, 7, 8, 1, 2
- [32] Chong Mou, Xintao Wang, Liangbin Xie, Yanze Wu, Jian Zhang, Zhongang Qi, and Ying Shan. T2i-adapter: Learning adapters to dig out more controllable ability for text-to-image diffusion models. In *Proceedings of the AAAI Conference on Artificial Intelligence*, pages 4296–4304, 2024. 3
- [33] Long Ouyang, Jeffrey Wu, Xu Jiang, Diogo Almeida, Carroll Wainwright, Pamela Mishkin, Chong Zhang, Sandhini Agarwal, Katarina Slama, Alex Ray, et al. Training language models to follow instructions with human feedback. Advances in neural information processing systems, 35:27730–27744, 2022. 1
- [34] Or Patashnik, Daniel Garibi, Idan Azuri, Hadar Averbuch-Elor, and Daniel Cohen-Or. Localizing object-level shape variations with text-to-image diffusion models. In *Proceedings of the IEEE/CVF International Conference on Computer Vision*, pages 23051–23061, 2023. 5
- [35] William Peebles and Saining Xie. Scalable diffusion models with transformers. In *Proceedings of the IEEE/CVF International Conference on Computer Vision*, pages 4195–4205, 2023. 1, 2
- [36] Alec Radford, Jong Wook Kim, Chris Hallacy, Aditya Ramesh, Gabriel Goh, Sandhini Agarwal, Girish Sastry, Amanda Askell, Pamela Mishkin, Jack Clark, et al. Learning transferable visual models from natural language supervi-

- sion. In *International conference on machine learning*, pages 8748–8763. PMLR. 2021. 5. 7
- [37] Colin Raffel, Noam Shazeer, Adam Roberts, Katherine Lee, Sharan Narang, Michael Matena, Yanqi Zhou, Wei Li, and Peter J Liu. Exploring the limits of transfer learning with a unified text-to-text transformer. *Journal of machine learning* research, 21(140):1–67, 2020. 5
- [38] Aditya Ramesh, Prafulla Dhariwal, Alex Nichol, Casey Chu, and Mark Chen. Hierarchical text-conditional image generation with clip latents. arXiv preprint arXiv:2204.06125, 1 (2):3, 2022. 1
- [39] Royi Rassin, Eran Hirsch, Daniel Glickman, Shauli Ravfogel, Yoav Goldberg, and Gal Chechik. Linguistic binding in diffusion models: Enhancing attribute correspondence through attention map alignment. Advances in Neural Information Processing Systems, 36, 2024. 2
- [40] Robin Rombach, Andreas Blattmann, Dominik Lorenz, Patrick Esser, and Björn Ommer. High-resolution image synthesis with latent diffusion models. In *Proceedings of the IEEE/CVF conference on computer vision and pattern recognition*, pages 10684–10695, 2022. 1, 2, 6
- [41] Olaf Ronneberger, Philipp Fischer, and Thomas Brox. Unet: Convolutional networks for biomedical image segmentation. In Medical image computing and computer-assisted intervention–MICCAI 2015: 18th international conference, Munich, Germany, October 5-9, 2015, proceedings, part III 18, pages 234–241. Springer, 2015. 1
- [42] Chitwan Saharia, William Chan, Saurabh Saxena, Lala Li, Jay Whang, Emily L Denton, Kamyar Ghasemipour, Raphael Gontijo Lopes, Burcu Karagol Ayan, Tim Salimans, et al. Photorealistic text-to-image diffusion models with deep language understanding. Advances in neural information processing systems, 35:36479–36494, 2022. 1, 2
- [43] Guibao Shen, Luozhou Wang, Jiantao Lin, Wenhang Ge, Chaozhe Zhang, Xin Tao, Yuan Zhang, Pengfei Wan, Zhongyuan Wang, Guangyong Chen, et al. Sg-adapter: Enhancing text-to-image generation with scene graph guidance. arXiv preprint arXiv:2405.15321, 2024. 3
- [44] Raphael Tang, Linqing Liu, Akshat Pandey, Zhiying Jiang, Gefei Yang, Karun Kumar, Pontus Stenetorp, Jimmy Lin, and Ferhan Ture. What the daam: Interpreting stable diffusion using cross attention. arXiv preprint arXiv:2210.04885, 2022. 2
- [45] Yoad Tewel, Rinon Gal, Gal Chechik, and Yuval Atzmon. Key-locked rank one editing for text-to-image personalization. In ACM SIGGRAPH 2023 Conference Proceedings, pages 1–11, 2023. 5
- [46] Hugo Touvron, Thibaut Lavril, Gautier Izacard, Xavier Martinet, Marie-Anne Lachaux, Timothée Lacroix, Baptiste Rozière, Naman Goyal, Eric Hambro, Faisal Azhar, et al. Llama: Open and efficient foundation language models. arXiv preprint arXiv:2302.13971, 2023. 1
- [47] A Vaswani. Attention is all you need. Advances in Neural Information Processing Systems, 2017. 1
- [48] Wenhai Wang, Enze Xie, Xiang Li, Deng-Ping Fan, Kaitao Song, Ding Liang, Tong Lu, Ping Luo, and Ling Shao. Pyramid vision transformer: A versatile backbone for dense

- prediction without convolutions. In *Proceedings of the IEEE/CVF international conference on computer vision*, pages 568–578, 2021. 1
- [49] Zijie J Wang, Evan Montoya, David Munechika, Haoyang Yang, Benjamin Hoover, and Duen Horng Chau. Diffusiondb: A large-scale prompt gallery dataset for text-toimage generative models. arXiv preprint arXiv:2210.14896, 2022. 2
- [50] Song Wen, Guian Fang, Renrui Zhang, Peng Gao, Hao Dong, and Dimitris Metaxas. Improving compositional text-to-image generation with large vision-language models. arXiv preprint arXiv:2310.06311, 2023. 2
- [51] Yan Xia, Hai Huang, Jieming Zhu, and Zhou Zhao. Achieving cross modal generalization with multimodal unified representation. Advances in Neural Information Processing Systems, 36, 2024.
- [52] Yang Zhang, Rui Zhang, Xuecheng Nie, Haochen Li, Jikun Chen, Yifan Hao, Xin Zhang, Luoqi Liu, and Ling Li. Spdiffusion: Semantic protection diffusion for multi-concept text-to-image generation. arXiv preprint arXiv:2409.01327, 2024. 3
- [53] Deyao Zhu, Jun Chen, Xiaoqian Shen, Xiang Li, and Mohamed Elhoseiny. Minigpt-4: Enhancing vision-language understanding with advanced large language models. *arXiv* preprint arXiv:2304.10592, 2023. 2
- [54] Jingyuan Zhu, Huimin Ma, Jiansheng Chen, and Jian Yuan. Isolated diffusion: Optimizing multi-concept text-to-image generation training-freely with isolated diffusion guidance. arXiv preprint arXiv:2403.16954, 2024. 2
- [55] Chenyi Zhuang, Ying Hu, and Pan Gao. Magnet: We never know how text-to-image diffusion models work, until we learn how vision-language models function. *arXiv preprint arXiv:2409.19967*, 2024. 3

Towards Transformer-Based Aligned Generation with Self-Coherence Guidance

Supplementary Material

6. Benchmark Details

To evaluate the capabilities of our model, we constructed a more comprehensive benchmark based on A&E [6]. Through our analysis, we identified that previous benchmarks primarily focused on coarse-grained attribute binding and lacked specific and complex scenarios. For example, prior benchmarks often evaluated prompts such as "a purple dog and a green bench." To address this limitation, we augmented the coarse-grained attribute binding tasks with specific place. For example, our prompts include cases such as "a green rabbit and a yellow bowl in the kitchen."

We argue that coarse-grained attribute binding alone is insufficient to comprehensively evaluate model performance. Therefore, we further extended the benchmark with fine-grained attribute binding and style binding tasks. Specifically, we manually created 56 fine-grained attribute binding prompts and 48 style binding prompts. Fine-grained attribute binding requires the model to control the attributes of different parts of a concept, while style prompts demand that multiple concepts within a single image exhibit distinct styles, the style prompts include categories such as "cyberpunk," "watercolor," "photorealistic," "anime," and others. The details of our benchmark is presented in Table 5.

For quantitative evaluation, we used metrics including text-to-text similarity and BLIP-VQA and additionally employed image-text similarity evaluation as discussed in section 8. Since both fine-grained attribute binding and style binding tasks involve only two concepts, we generated two questions per prompt for BLIP-VQA evaluation. For coarse-grained attribute binding tasks, as the generated image must adhere to specific locations, we generated three questions per prompt. For example, given the prompt "a blue dog and a red bench in the street," the corresponding questions are: "a blue dog?", "a red bench?", and "the street?"

This enhanced benchmark allows for a more comprehensive evaluation of model capabilities across coarse-grained, fine-grained, and style attribute bindings. Our evaluation was conducted on RTX 3090 GPUs, with each generation taking approximately 20 seconds.

7. Algorithm Details

The process of our method is detailed in Algorithm 1. Specifically, the SCG function corresponds to the approach for obtaining the new attention map described in Equation 2.

Algorithm 1 Self-Coherence Guidance.

Input: A text prompt \mathcal{P} , random seed s and hyper-parameter c.

Output: The latent space z_0 corresponding to images with strong consistency to the text prompt \mathcal{P} .

```
1: for t = T, T - 1, \dots, 1 do
            z_{t-1}^*, A_t \leftarrow DM(z_t, t)
            M_t \leftarrow Cluster(A_t)/LLMplanning(A_t)
 3:
 4:
            for n = 1, 2, ..., N do
 5:
                  A_t^n \leftarrow TransBlock^n(h^{n-1})
\widehat{A_t^n} \leftarrow SCG(A_t^n, M_{t+1}, c)
h^n \leftarrow TransBlock^n(h^{n-1})\{A_t^n \leftarrow \widehat{A_t^n}\}
 6:
 7:
 8:
 9:
            end for
            z_{t-1} = h^N
11: end for
12: Return z_0
```

Here, N represents the number of Transformer blocks, h represents the hidden state that each Transformer block outputs, M_t represents the masks of the concepts extracted for the next step. We iteratively replace the original attention maps with the new attention maps for each block.

8. More Quantitative Results

To further quantitatively evaluate the performance of our method, we employed image-text similarity as a metric. Following [6, 31], we utilized CLIP to separately encode images and their corresponding textual descriptions and computed their similarity scores, as shown in the Fig. 7. In this evaluation, "Full Prompts" similarity refers to the similarity between the complete prompt and the image, while "Minimum Object" similarity measures the similarity between the image and the neglected half of the text prompt.

Our method consistently outperforms previous approaches across all three tasks, with significant improvements in average similarity for both coarse-grained and finegrained attribute binding. Notably, while the CONFORM achieves results close to ours on coarse-grained attribute binding, it fails to generalize effectively to fine-grained attribute binding and style binding, showing the poorest performance in the latter. The original PIXART- α model performs reasonably well on fine-grained attribute binding, and our approach further enhances its performance, achieving

Table 5. The details of our benchmark. BLIP-VQA refers to the number of generated questions when evaluated using the BLIP-VQA metric.

Task		Template & Example		Pr	ompt number	BLIP-VQA
Coarse-grained	'a ble a [colorA][conce	a [colorA][conceptA] and a [colorB][conceptB] 'a black backpack and a pink balloon' a [colorA][conceptA] and a [colorB][conceptB] in the [place] 'a blue rabbit and a yellow bowl in the kitchen'			54	3
Fine-grained			partA] and a [colorB][parge stem and blue flesh'	tB]	56	2
Style			nd a [sytleB][conceptB] hotorealistic kitchen'		48	2
0.40	oarse-grained	0.40	Fine-grained	0.40	Sty	/le
0.35 -		0.35 -		0.35 -	_	
0.30 -		0.30 -		0.30 -		
0.25 -		0.25 -		0.25 -		
0.25 - 0.20 - 0.15 -		0.20 -		0.20 -		
0.15 -		0.15 -		0.15 -		
0.10 -		0.10 -		0.10 -		
0.05 -		0.05 -		0.05 -		
0.00	t Minimum Object	0.00	ull Prompt Minimum Object	0.00	Full Prompt	Minimum Object

Figure 7. Comparison of average image-text similarity across different tasks. We compare our proposed method with the original PIXART- α model and two state-of-the-art aligned generation methods built on SD: D&B and CONFORM.

the best results. However, for style binding, the improvement of our method over D&B is relatively modest.

We attribute this limitation to the BLIP-caption model, which lacks specialized training for style-specific images. Consequently, it struggles to capture the fine-grained stylistic details of different concepts in images, demonstrating insensitivity to style.

In addition, we also employed the evaluation metric VQAScore. VQAScore is similar to the BLIP-VQA metric, as both assess image-text alignment by leveraging a VQA model. As shown in table 6. Our method achieves SOTA results on this additional metric as well.

To achieve a more accurate analysis, we provide a more comprehensive qualitative evaluation in the following section.

Table 6. Comparison of VQAScore. Our method still achieves state-of-the-art performance on this metric.

Method	Coarse-grained	Fine-grained	Style
D&B(SD) [23]	0.372	0.342	0.307
CONFORM(SD) [31]	0.412	0.376	0.312
PIXART- α [7]	0.387	0.437	0.320
Ours	0.476	0.488	0.366

9. Ablation Study

We conduct ablation studies to compare the performance of LLM and K-means approaches. Specifically, we evaluate both methods across three tasks: coarse-grained attribute binding, fine-grained attribute binding, and style binding. BLIP-VQA is used as the evaluation metric. The results are shown in table 7. Our experimental results demonstrate that the LLM-based approach performs better on the fine-



Figure 8. The experimental results on Flux demonstrate that our method remains effective under the MMDiT architecture..

grained attribute binding task. We attribute this to the following three reasons. **First**, the saliency of attention maps varies across different tasks, with fine-grained tasks exhibiting the least salient attention maps. **Second**, clustering algorithms process signals directly from the model output, whereas LLMs incorporate external knowledge to assist in interpreting the output. As a result, when the attention map is highly salient, clustering algorithms achieve better performance. **Finally**, LLMs provide additional benefits only when the attention map lacks saliency, making them more effective in fine-grained tasks.

Table 7. Ablation study comparing different grouping strategies.

Method	Coarse-grained	Fine-grained	Style
w/ LLM	0.647	0.623	0.781
w/ K-means	0.679	0.613	0.799

10. Generalizability

To verify the generalization capability of our method, we further conduct experiments on Flux [1]. Unlike PIXART- α [7], Flux [1] adopts the MMDiT architecture, which concatenates the QKV of text and image modalities before computing attention. In this setting, we still treat the dot product between the image queries and text keys as the cross-attention map on which our method operates. As shown in Fig 8, our approach remains effective under the MMDiT architecture, demonstrating strong generalization ability.

11. More Qualitative Results

To further validate the effectiveness of our approach, we provide additional qualitative analysis results for fine-grained attribute binding, style binding, and coarse-grained attribute binding tasks. These results further validate the effectiveness of our method.

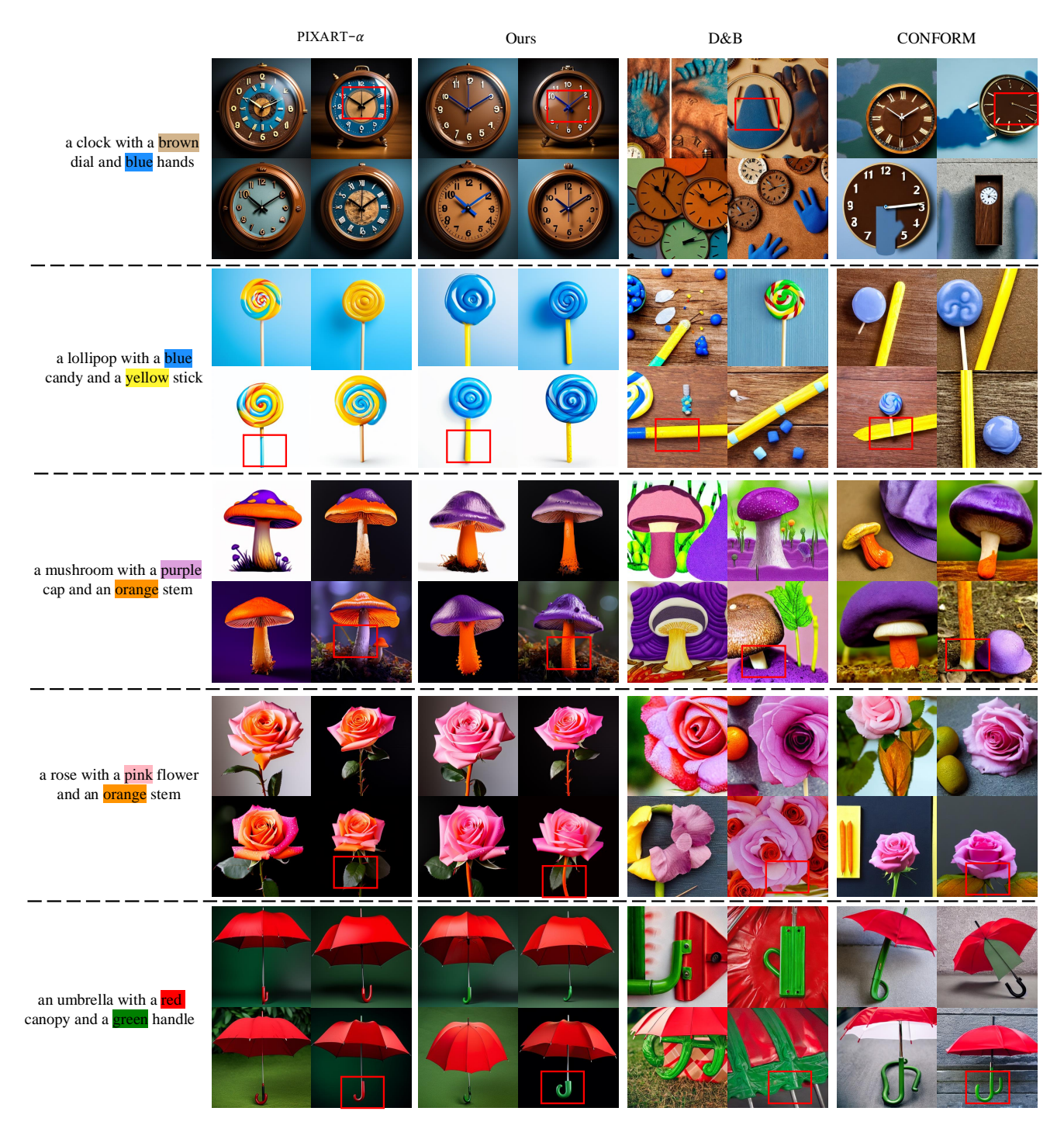


Figure 9. Qualitative analysis of fine-grained attribute binding comparing our method with other SOTA approaches. Our method enables more precise control over the attributes of concepts.

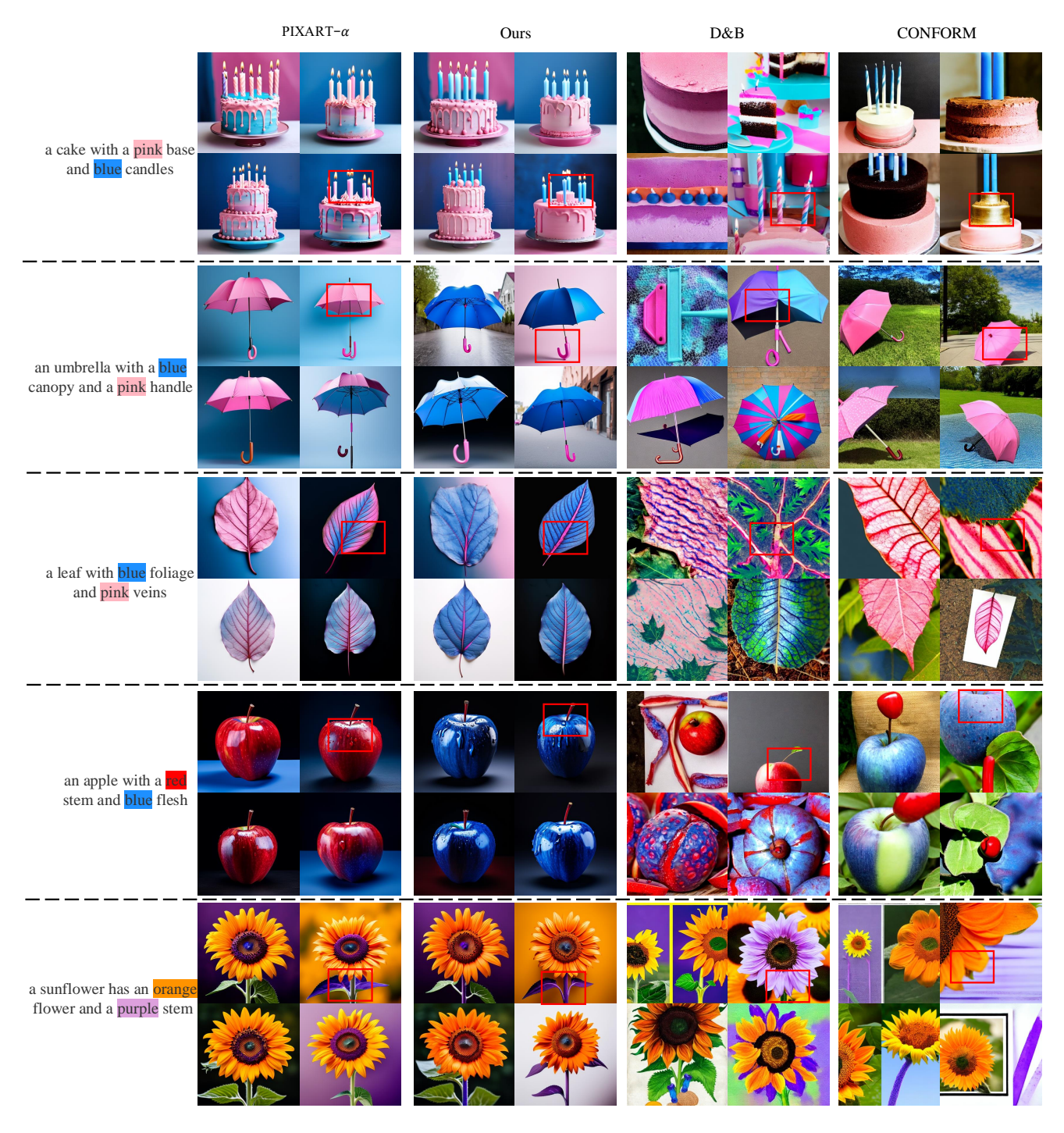


Figure 10. Qualitative analysis of fine-grained attribute binding comparing our method with other SOTA approaches. Our method enables more precise control over the attributes of concepts.



Figure 11. Qualitative analysis of style binding comparing our method with other SOTA approaches. Our method effectively binds styles to different concepts.

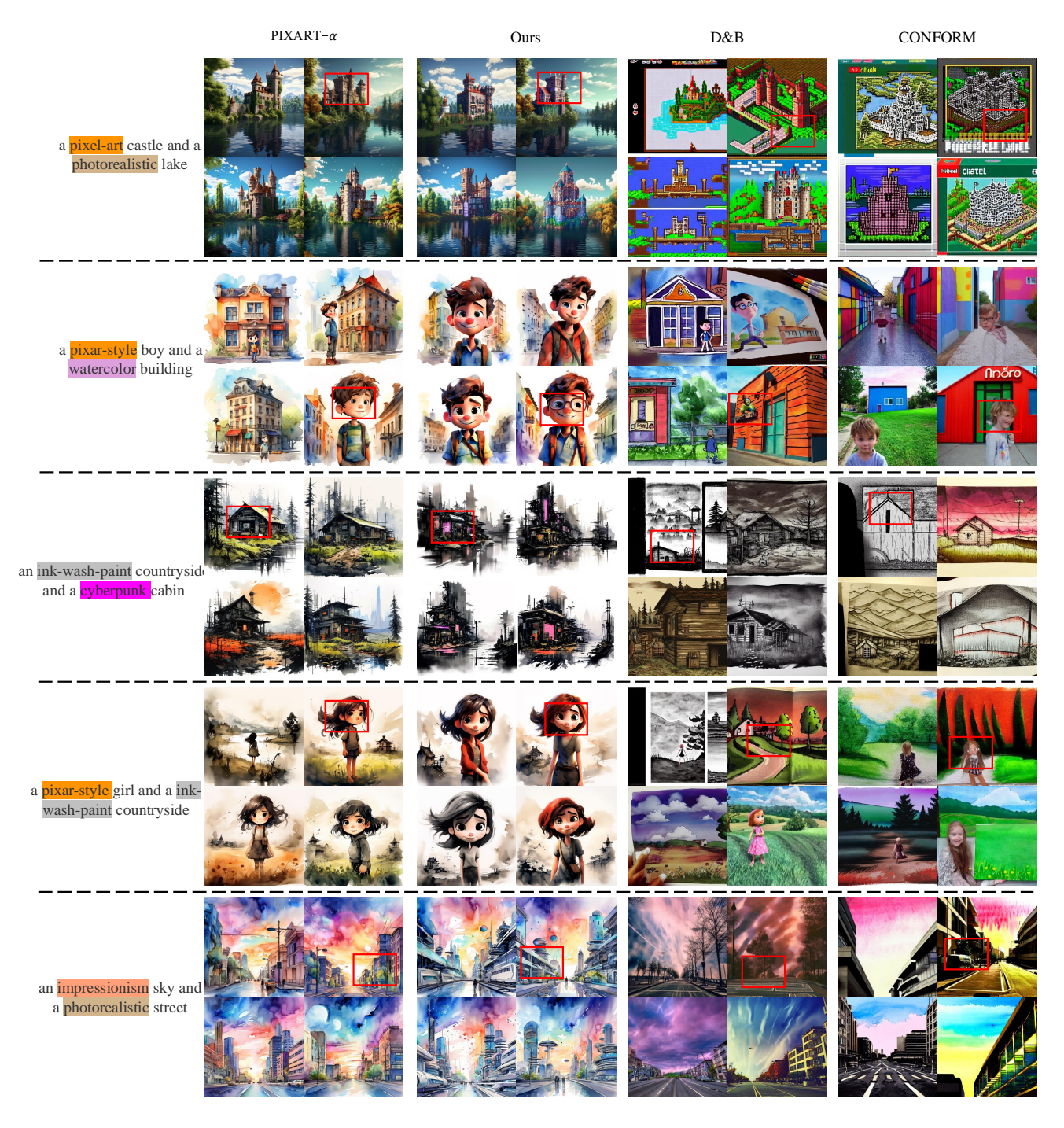


Figure 12. Qualitative analysis of style binding comparing our method with other SOTA approaches. Our method effectively binds styles to different concepts.

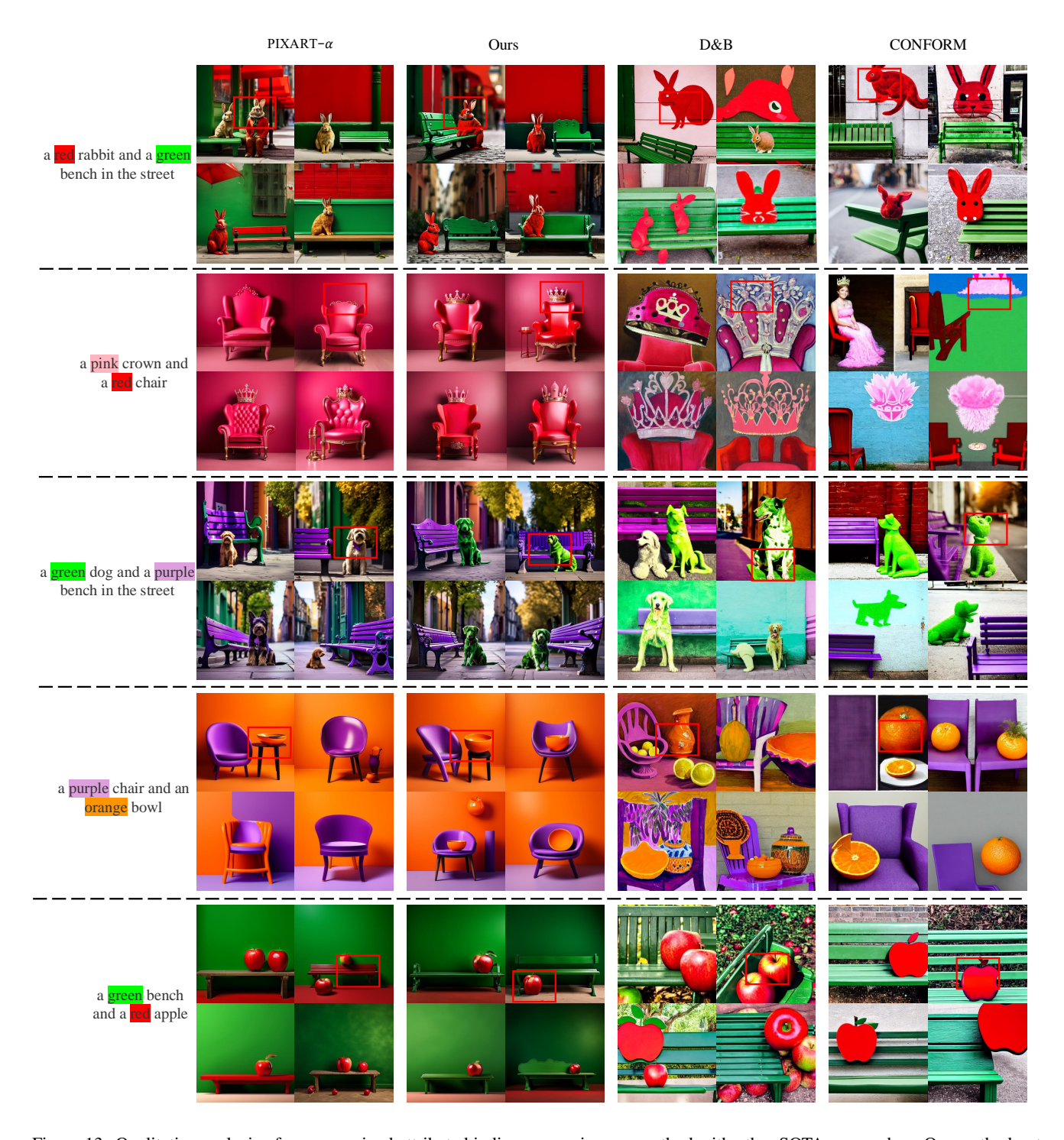


Figure 13. Qualitative analysis of coarse-grained attribute binding comparing our method with other SOTA approaches. Our method not only achieves attribute control but also generates higher-quality concepts.

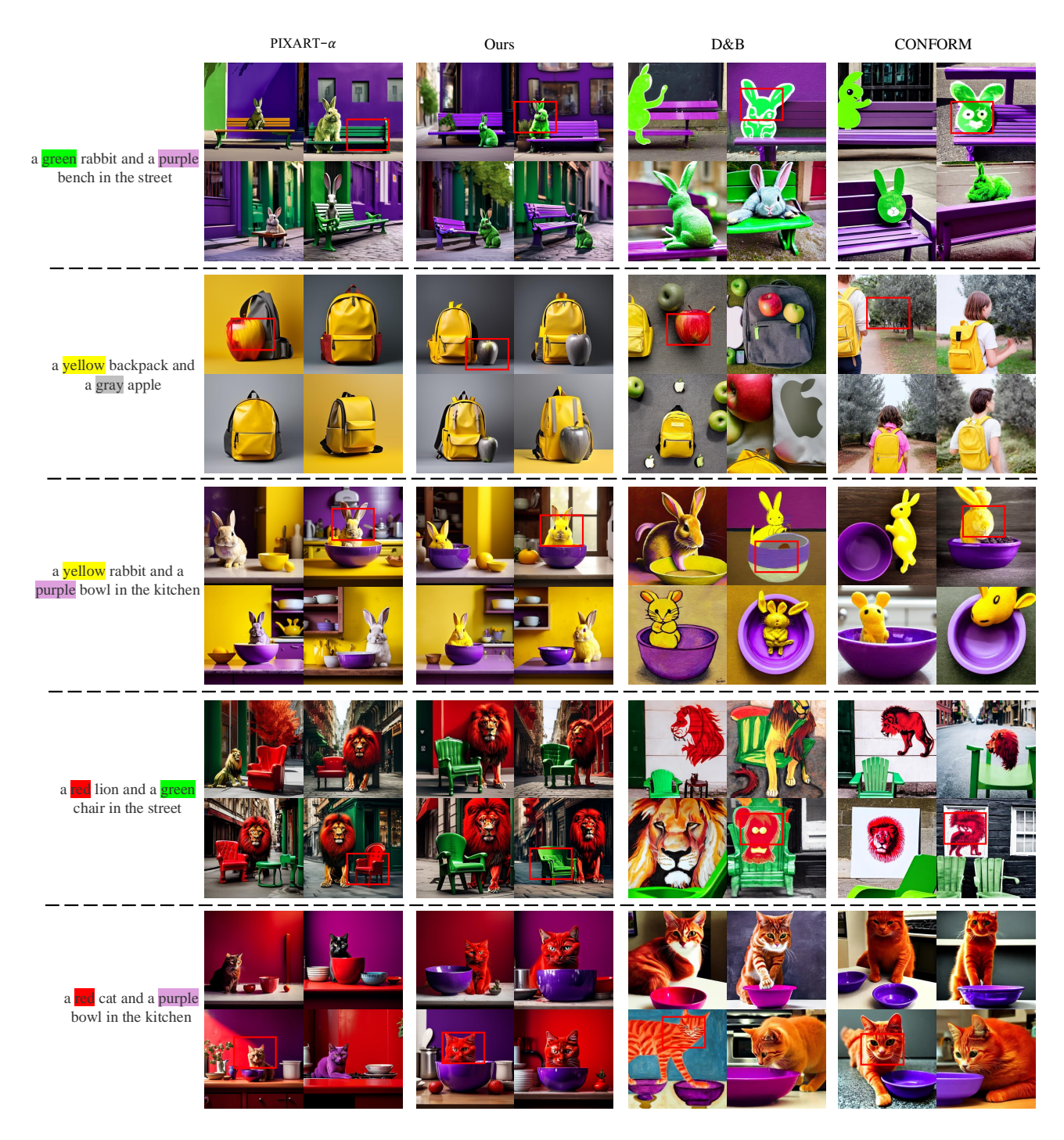


Figure 14. Qualitative analysis of coarse-grained attribute binding comparing our method with other SOTA approaches. Our method not only achieves attribute control but also generates higher-quality concepts.